A R C H I V E O F M E C H A N I C A L E N G I N E E R I N G

VOL. LXV 2018 Number 3

DOI: 10.24425/124485

Key words: speed-dependent dynamic parameters, rotor-bearing-coupling, misalignment, analytical approach, multiple-faults, Lagrange's method

MOHIT LAL [1], *MONALISHA SATAPATHY*[1]

ESTIMATION OF SPEED DEPENDENT FAULT PARAMETERS IN A COUPLED ROTOR-BEARING SYSTEM

In rotating machineries, misalignment is considered as the second most major cause of failure after unbalance. In this article, model-based multiple fault identification technique is presented to estimate speed-dependent coupling misalignment and bearing dynamic parameters in addition with speed independent residual unbalances. For brevity in analysis, a simple coupled rotor bearing system is considered and analytical approach is used to develop the identification algorithm. Equations of motion in generalized co-ordinates are derived with the help of Lagrange's equation and least squares fitting approach is used to estimate the speed-dependent fault parameters. Present identification algorithm requires independent sets of forced response data which are generated with the help of different sets of trial unbalances. To avoid/suppress the ill-conditioning of regression equation, independent sets of forced response data are obtained by rotating the rotor in clock-wise and counter clock-wise directions, alternatively. Robustness of algorithm is checked for different levels of measurement noise.

1. Introduction

In the present scenario, rotating machineries play a vital role in most of the industries. Even a small disturbance/fault in rotating machineries may cause huge economic loss as well as hazardous effects on human life. Hence, a precise and reliable estimation of dynamic parameters (related with different faults) of rotating machineries are needed. Apart from various faults associated with rotating machineries, speed-dependent faults (mainly coupling misalignment faults) have not attracted as many researchers as it actually requires. Although some researchers have estimated speed independent bearing-coupling parameters and speed-dependent bearing dynamic parameters, but the literature counts in the esti-

[1] *Department of Industrial Design, National Institute of Technology Rourkela, 769008 Rourkela, Odisha, India. Emails: lalm@nitrkl.ac.in, 615ID1002@nitrkl.ac.in*

mation of speed-dependent coupling parameters are nearly negligible (some have considered time dependency in the coupling parameters [1]). The importance and necessity of considering speed dependency in estimation of coupling misalignment parameters are discussed in article [2].

An identification methodology is developed to estimate speed-dependent bearing parameters to represent bearing faults by authors of [3]. They proposed combination of regularization and generalized singular value decomposition technique to improve the accuracy of developed methodology by improving condition number of the regression matrix. In Ref. [4], the influence of parallel misalignment on lateral and torsional response of rotor system is analyzed. The authors used combination of the Newmark and Newton-Raphson method to analyze the transient response of the system. Authors of [5] studied the effect of angular misalignment on stability region of coupled rotor system and concluded that angular misalignment increases the instability region. A methodology to estimate the bearing parameters and residual unbalance simultaneously is developed in [6]. The authors proposed three novel techniques to improve the condition number of regression matrix. Authors of [7] proposed a methodology based on impulse response measurement to estimate residual unbalances and speed-dependent bearing parameters, simultaneously. A review on various fault detection techniques is performed by authors of [8]. They mainly focused on faults related to rolling contact bearing and suggested that the wavelets and Hilbert transform might be useful in fault signature analysis. Residual information of the system is utilized to identify faults in rotating machineries in [9]. The authors mainly focused on the modelling of unbalance and misalignment present in rotor system. A discussion on the developments in model-based condition monitoring techniques is presented in article [10]. Authors of [11] analyzed the combined effects of parallel misalignment and unbalance on the response and concluded that significant effect of misalignment can be seen in most of the speeds except at high speeds. A novel approach (Blind Source Separation) to separate the vibrational features generated due to various faults present in rotor system is proposed by authors of [12]. They concluded Blind Source Separation is feasible and supportive for multi-fault diagnosis. An analysis on axial, lateral and torsional vibration is presented in Ref. [13, 14]. The authors concluded that different modes are coupled due to misalignment.

Authors of [15] used Lagrange multiplier to model parallel, angular and combined misalignment condition and performed two-step nonlinear FE analysis. Flexibility disassembly method to identify the structural damages is proposed by authors of [16]. They estimated the flexibility parameters, exactly. Article [17] discussed about three different methods to identify unbalance and reported well agreement between the numerical and experimental results. Dynamic characteristics of a flexible diaphragm coupling with parallel misalignment are examined in [18]. The authors considered time dependent stiffness (direct as well as cross–coupled) parameters to model the coupling.

Misalignment is modelled in terms of equivalent stiffness and damping of coupling to estimate misalignment force and moments by authors of [19, 20]. They used analytical (Lagrange's approach) to obtain system equations of motion. Later authors of [2] extended the work carried out by authors of [19] by using more practical solution approach, i.e., finite element approach and found out the bearing and coupling dynamic parameters along with residual unbalances. Work of authors [2] is supported with experimental results by authors of [21–23]. They also proposed a novel condensation (high frequency condensation) technique to reduce the degrees of freedom of the system. The effects of radial and angular misalignments in a hyper–static shaft line mounted on fluid–film journal bearings are studied in [24]. The authors used Reynolds equations to model fluid film bearings. A review on different faults such as gear fault, rotor fault and bearing fault in rotating machineries is performed in [25]. The authors concluded Empirical Mode Decomposition technique can be used as a tool to diagnose these faults. Active magnetic bearing along with proportional integral derivative controller is used to diagnose misaligned system in Ref. [26]. Authors of [26] estimated misalignment parameters along with dynamic parameters of active magnetic bearing and proportional integral derivative controller.

Based on literature survey discussed above, it is evident that the more appropriate modelling of turbo–generator system is lacking. This lacking/gap could be filled by considering the speed-dependent bearing and coupling dynamic parameters together in the modelling. In this article, an identification algorithm is developed to estimate speed-dependent coupling and bearing dynamic parameters that represents misalignment and bearing fault, respectively, in addition with residual unbalances. Model description along with assumptions involved to develop identification algorithm is presented in the next section.

2. Theoretical development

Present section concerns with the assumptions involved to model the coupled rotor bearing system.

2.1. Assumptions involved and model description

To have more insight into the modelling of speed-dependent fault parameters, a very basic/simple model is considered at present. Two massless rigid shafts having a rigid disc at its mid-span, connected together with a flexible coupling and mounted over flexible bearings at ends is considered in this analysis, whereas the assumption of basic model could be overcome by considering more realistic flexible shaft model with defined shaft modelling techniques such as Timoshenko beam theory and Euler-Bernoulli beam theory. An abstract view of the coupled rotor bearing system considered to develop an identification algorithm is shown in Fig. 1. Deflected position of rotor system along the $(z–x)$ plane is delineated

in Fig. 2. Here b_1 to b_4 represent the bearing positions, d_1 and d_2 represent the disc positions, and (u, φ_v) represent the linear and angular displacements of the rotor in $(z–x)$ plane, respectively. Disc properties considered are mass, m_i^d, the diametral moment of inertia, I_i^d, and residual unbalance F_i^{res} (where $i = 1$, 2; number of discs). Bearings are modelled as having eight linearized stiffness, $k_{ij}^{b_m}$, and damping, $c_{ij}^{b_m}$, coefficients (Each bearing is having dissimilar direct and cross–coupled terms i.e. i, $j = u$, v; where $m = 1$, 2, 3, 4, number of bearings). Also, flexible coupling is modelled as having eight linearized stiffness (k_{ij}^c) and damping (c_{ij}^c) along with two rotational stiffness ($k_{\varphi_i}^c$, $k_{\varphi_j}^c$) coefficient (where i, $j = u$, v). Superscripts b, c, and d represent bearing, coupling and disc, respectively.

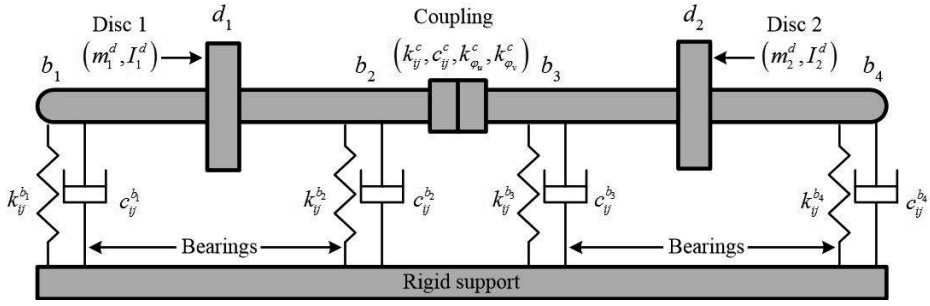

Fig. 1. A schematic diagram of turbo-generator system

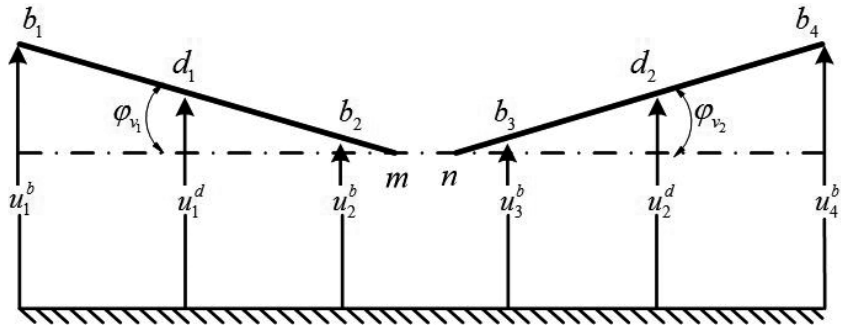

Fig. 2. Turbo-generator system in a deflected position in $(z - x)$ plane

2.2. Equations of motion

Linear displacements $\left(u_i^b, v_i^b\right)$ at bearing locations in two orthogonal directions are considered as generalized co-ordinates to obtain equations of motion. All the linear and angular displacements at different axial locations in the shaft could be

obtained in terms of generalized coordinates as

$$\begin{aligned}
u_1^d &= 0.50(u_1^b + u_2^b); \quad u_2^d = 0.50(u_3^b + u_4^b);\\
v_1^d &= 0.50(v_1^b + v_2^b); \quad v_2^d = 0.50(v_3^b + v_4^b);\\
\varphi_{v_1} &= \frac{1}{l_1}(u_1^b - u_2^b); \quad \varphi_{v_2} = \frac{1}{l_2}(u_4^b - u_3^b);\\
\varphi_{u_1} &= \frac{1}{l_1}(v_1^b - v_2^b); \quad \varphi_{u_2} = \frac{1}{l_2}(v_4^b - v_3^b);\\
u_1^c &= (-0.25u_1^b + 1.25u_2^b); \quad u_2^c = (1.25u_3^b - 0.25u_4^b);\\
v_1^c &= (-0.25v_1^b + 1.25v_2^b); \quad v_2^c = (1.25v_3^b - 0.25v_4^b).
\end{aligned} \tag{1}$$

The total length of each shaft is $1.25l$, where $0.25l$ is the overhang length in each shaft towards the coupling. With the help of above displacements, kinetic energy of the system and virtual work done due to different forces (stiffness, damping and unbalance) could be obtained. Kinetic energy (T) could be represented as

$$\begin{aligned}
T = \frac{1}{2}m_1^d(\dot{u}_1^d)^2 + \frac{1}{2}m_2^d(\dot{u}_2^d)^2 + \frac{1}{2}I_1\dot{\varphi}_{v_1}^2 + \frac{1}{2}I_2\dot{\varphi}_{v_2}^2 + \frac{1}{2}m_1^d(\dot{v}_1^d)^2\\
+ \frac{1}{2}m_2^d(\dot{v}_2^d)^2 + \frac{1}{2}I_1\dot{\varphi}_{u_1}^2 + \frac{1}{2}I_2\dot{\varphi}_{u_2}^2\,.
\end{aligned} \tag{2}$$

Virtual work could be represented as

$$\delta W = \delta W_{stiff} + \delta W_{damp} + \delta W_{unb} \tag{3}$$

with

$$\begin{aligned}
\delta W_{stiff} = &-k_{uu}^{b_1}u_1^b\delta u_1^b - k_{uv}^{b_1}v_1^b\delta u_1^b - k_{vu}^{b_1}u_1^b\delta v_1^b - k_{vv}^{b_1}v_1^b\delta v_1^b - k_{uu}^{b_2}u_2^b\delta u_2^b\\
&- k_{uv}^{b_2}v_2^b\delta u_2^b - k_{vu}^{b_2}u_2^b\delta v_2^b - k_{vv}^{b_2}v_2^b\delta v_2^b - k_{uu}^{b_3}u_3^b\delta u_3^b - k_{uv}^{b_3}v_3^b\delta u_3^b - k_{vu}^{b_3}u_3^b\delta v_3^b\\
&- k_{vv}^{b_3}v_3^b\delta v_3^b - k_{uu}^{b_4}u_4^b\delta u_4^b - k_{uv}^{b_4}v_4^b\delta u_4^b - k_{vu}^{b_4}u_4^b\delta v_4^b - k_{vv}^{b_4}v_4^b\delta v_{b_4}\\
&- k_{uu}^c(u_1^c - u_2^c)\delta(u_1^c - u_2^c) - k_{uv}^c(v_1^c - v_2^c)\delta(u_1^c - u_2^c)\\
&- k_{vu}^c(u_1^c - u_2^c)\delta(v_1^c - v_2^c) - k_{vv}^c(v_1^c - v_2^c)\delta(v_1^c - v_2^c)\\
&- k_{\varphi_u}^c(\varphi_{u_1}^c - \varphi_{u_2}^c)\delta(\varphi_{u_1}^c - \varphi_{u_2}^c) - k_{\varphi_v}^c(\varphi_{v_1}^c - \varphi_{v_2}^c)\delta(\varphi_{v_1}^c - \varphi_{v_2}^c),
\end{aligned} \tag{4}$$

$$\begin{aligned}
\delta W_{damp} = &-c_{uu}^{b_1}\dot{u}_1^b\delta u_1^b - c_{uv}^{b_1}\dot{v}_1^b\delta u_1^b - c_{vu}^{b_1}\dot{u}_1^b\delta v_1^b - c_{vv}^{b_1}\dot{v}_1^b\delta v_1^b - c_{uu}^{b_2}\dot{u}_2^b\delta u_2^b\\
&- c_{uv}^{b_2}\dot{v}_2^b\delta u_2^b - c_{vu}^{b_2}\dot{u}_2^b\delta v_2^b - c_{vv}^{b_2}\dot{v}_2^b\delta v_2^b - c_{uu}^{b_3}\dot{u}_3^b\delta u_3^b - c_{uv}^{b_3}\dot{v}_3^b\delta u_3^b - c_{vu}^{b_3}\dot{u}_3^b\delta v_3^b\\
&- c_{vv}^{b_3}\dot{v}_3^b\delta v_3^b - c_{uu}^{b_4}\dot{u}_4^b\delta u_4^b - c_{uv}^{b_4}\dot{v}_4^b\delta u_4^b - c_{vu}^{b_4}\dot{u}_4^b\delta v_4^b - c_{vv}^{b_4}\dot{v}_4^b\delta v_4^b\\
&- c_{uu}^c(\dot{u}_1^c - \dot{u}_2^c)\delta(u_1^c - u_2^c) - c_{uv}^c(\dot{v}_1^c - \dot{v}_2^c)\delta(u_1^c - u_2^c)\\
&- c_{vu}^c(\dot{u}_1^c - \dot{u}_2^c)\delta(v_1^c - v_2^c) - c_{vv}^c(\dot{v}_1^c - \dot{v}_2^c)\delta(v_1^c - v_2^c)
\end{aligned} \tag{5}$$

and

$$\delta W_{unb} = F_i^x(t)\delta(u_1^c + 0.75l\varphi_{v_1}) + F_i^x(t)\delta(u_2^c + 0.75l\varphi_{v_2}) + F_i^y(t)\delta(v_1^c + 0.75l\varphi_{u_1}) + F_i^y(t)\delta(v_2^c + 0.75l\varphi_{u_2}), \tag{6}$$

where F_i^x and F_i^y denotes the unbalance forces in the $(x–z)$ and $(y–z)$ planes, respectively. The unbalance force in two planes could be related as $F_i^y = \pm j\, F_i^x$ (+ and − sign indicates counter-clockwise and clockwise rotation of the rotor, respectively). Residual unbalance forces are taken in the form of $F_i^{res} = U_i^{res}\omega^2 e^{j(\omega t+\phi_i)}$ with $U_i^{res} = m_i^{res} e_i$ where, m_i^{res} and e_i are the mass and eccentricity of residual unbalance, respectively $(i = 1, 2)$. ϕ_i is the phase of residual unbalance against a point of reference on the shaft and δ is the functional operator. The kinetic energy and virtual work done could be used in Lagrange's equation to obtain the equations of motion and could be written as,

$$[M]\{\ddot{\eta}\} + [C]\{\dot{\eta}\} + [K]\{\eta\} = \{f(t)\}, \tag{7}$$

with

$$\{f(t)\} = \omega^2 \begin{Bmatrix} 0.50F_1^{res}e^{j\phi_1} \\ 0.50F_1^{res}e^{j\phi_1} \\ 0.50F_2^{res}e^{j\phi_2} \\ 0.50F_2^{res}e^{j\phi_2} \\ -j0.50F_1^{res}e^{j\phi_1} \\ -j0.50F_1^{res}e^{j\phi_1} \\ -j0.50F_2^{res}e^{j\phi_2} \\ -j0.25F_2^{res}e^{j\phi_2} \end{Bmatrix} e^{j\omega t}; \qquad \{\eta(t)\} = \begin{Bmatrix} u_1^b(t) \\ u_2^b(t) \\ u_3^b(t) \\ u_4^b(t) \\ v_1^b(t) \\ v_2^b(t) \\ v_3^b(t) \\ v_4^b(t) \end{Bmatrix}.$$

Detailed information of matrices $[M]$, $[K]$ and $[C]$ is presented in Appendix A. In Eq. (7), force has the complex form as $\{f(t)\} = \left\{\overline{f}\right\} e^{j\omega t}$. Hence, upon assuming the solution in the form of $\{\eta(t)\} = \{\overline{\eta}\}\, e^{j\omega t}$, Eq. (7) could be obtained in frequency domain as,

$$\left([K] + j\omega[C] - \omega^2[M]\right)\{\overline{\eta}\} = \left\{\overline{f}\right\}. \tag{8}$$

To obtain independent sets of force response data, Eq. (8) could be used for known system information. Further, these generated responses are used in regression equation to formulate identification algorithm to estimate speed-dependent fault parameters. The form of regression equation could be obtained by rearranging Eq. (8), in such a manner that all the unknown quantities (stiffness and damping parameters of bearing and coupling and residual unbalances) and the corresponding coefficients

are stacked in left hand side vector and matrix, respectively, and all the known quantities (mass and diametral moment of inertia) are stacked in right hand side vector. Such reframed equation in complex form for one spin speed could be expressed as,

$$[A_1(\omega)]_{8\times44}\{X_1\}_{44\times1} = \{B_1(\omega)\}_{8\times1}\,. \tag{9}$$

After separating out the real and imaginary terms for one spin speed Eq. (9), could be expressed as

$$[A_2(\omega)]_{16\times46}\{X_2\}_{46\times1} = \{B_2(\omega)\}_{16\times1}\,, \tag{10}$$

with

$$\begin{aligned}\{X_2\}_{46\times1} = \{&k^{b_1}_{uu}, k^{b_1}_{uv}, k^{b_1}_{vu}, k^{b_1}_{vv}, k^{b_2}_{uu}, k^{b_2}_{uv}, k^{b_2}_{vu}, k^{b_2}_{vv}, k^{b_3}_{uu}, k^{b_3}_{uv}, k^{b_3}_{vu}, k^{b_3}_{vv}, k^{b_4}_{uu}, k^{b_4}_{uv},\\ &k^{b_4}_{vu}, k^{b_4}_{vv}, k^{c}_{uu}, k^{c}_{uv}, k^{c}_{vu}, k^{c}_{vv}, k^{c}_{\varphi_u}, k^{c}_{\varphi_v}, c^{b_1}_{uu}, c^{b_1}_{uv}, c^{b_1}_{vu}, c^{b_1}_{vv}, c^{b_2}_{uu}, c^{b_2}_{uv},\\ &c^{b_2}_{vu}, c^{b_2}_{vv}, c^{b_3}_{uu}, c^{b_3}_{uv}, c^{b_3}_{vu}, c^{b_3}_{vv}, c^{b_4}_{uu}, c^{b_4}_{uv}, c^{b_4}_{vu}, c^{b_4}_{vv}, c^{c}_{uu}, c^{c}_{uv}, c^{c}_{vu}, c^{c}_{vv},\\ &f^{res}_{1_{real}}, f^{res}_{1_{imag}}, f^{res}_{2_{real}}, f^{res}_{2_{imag}}\}^{\mathrm{T}};\end{aligned}$$

$$[A_2(\omega)]_{16\times46} = \left[[K^R]_{16\times22}\ \ [C^R]_{16\times20}\ \ [F^R]_{16\times4}\right]_{16\times46};$$

$$\left[K^R\right]_{16\times22} = \begin{bmatrix}\left[K^R_{real}\right]_{8\times22}\\ \left[K^R_{img}\right]_{8\times22}\end{bmatrix}_{16\times22}; \qquad \left[C^R\right]_{16\times20} = \begin{bmatrix}\left[C^R_{real}\right]_{8\times20}\\ \left[C^R_{img}\right]_{8\times20}\end{bmatrix}_{16\times20};$$

$$\left[F^R\right]_{16\times4} = \begin{bmatrix}\left[F^R_{real}\right]_{8\times4}\\ \left[F^R_{img}\right]_{8\times4}\end{bmatrix}_{16\times4},$$

where $\{X\}$ is the vector of unknown quantities, $[A]$ is coefficient matrix having the response information corresponding to stiffness $[K^R]$, damping $[C^R]$ and unbalance $[F^R]$. $\{B\}$ is the vector of known quantities. Subscripts used in Eq. (10), represent the size of individual matrix and vector.

As it could be noticed from Eq. (10), the number of unknown quantities, i.e., forty-six is greater than the number of equations, i.e. sixteen, this leads to the underdetermined system of liner simultaneous equations. In order to make the system of equations determined, minimum three sets of independent response are required. Since the objective of the present article is to estimate speed-dependent fault parameters, the conventional techniques used by authors of [19] to make the system determined by varying speeds are not applicable. Hence, different sets of trial unbalances at one speed are used in this analysis to obtain independent force-response data and to make the system at least determined or over-determined [6]. However, the accuracy of estimated parameters highly depends upon the condition number of the regression matrix to be inverted. In the succeeding section, different ways to achieve determined system of equations and procedures to improve the condition of the regression matrix are deliberated.

3. Conditioning of regression matrix

Different possibilities to obtain independent sets of force–response data to improve the condition number of the regression matrix are discussed in this section:

- *Case A*: with three sets of measurement, i.e., exactly determined case;
- *Case B*: with more (eight) sets of measurement, i.e., highly over–determined case.

To see the effect of forward and backward whirl in the estimated parameters, the above cases are analyzed under a condition in which rotor rotates in clockwise and counter-clockwise directions, alternatively. Despite of rotating the rotor only in one direction, alternate rotor rotation in clockwise and counter clockwise direction is generally suggested for well-conditioning of the regression matrix [7]. To obtain better estimates, regression equation Eq. (10), could be expressed as,

$$[A_3(\omega)]_{(16\times m)\times 46}\{X_3\}_{46\times 1} = \{B_3(\omega)\}_{(16\times m)\times 1}\,, \tag{11}$$

with

$$[A_3(\omega)]_{(16\times m)\times 46} = \begin{bmatrix} [A_{3a_1}(\omega)]_{16\times 46} \\ [A_{3a_2}(-\omega)]_{16\times 46} \\ \vdots \\ [A_{3a_{m-1}}(\omega)]_{16\times 46} \\ [A_{3a_m}(-\omega)]_{16\times 46} \end{bmatrix}_{(16\times m)\times 46};$$

$$[B_3(\omega)]_{(16\times m)\times 1} = \begin{bmatrix} [B_{3a_1}(\omega)]_{16\times 1} \\ [B_{3a_2}(-\omega)]_{16\times 1} \\ \vdots \\ [B_{3a_{m-1}}(\omega)]_{16\times 1} \\ [B_{3a_m}(-\omega)]_{16\times 1} \end{bmatrix}_{(16\times m)\times 1},$$

where A_3 and B_3 have the same form as A_2 and B_2, respectively, as in Eq. (10) with different possibilities of trial unbalances ($m = 3, 8$; for *Case A* and *Case B*, respectively) at one speed, alternatively in clockwise and counter-clockwise directions. Next section, discusses about the development of identification methodology to estimate speed-dependent fault parameters.

4. Formulation of identification methodology

Eq. (11), is the regression equation with determined system of equations under *Case A* and *Case B* at one speed for speed independent bearing and coupling dynamic parameters. The generalized form of regression equation to estimate speed-dependent dynamic fault parameters could be written as

$$[A(\omega)]_{((16\times m\times n)\times(42\times n+4))}\{X(\omega)\}_{((42\times n+4)\times 1)} = \{B(\omega)\}_{((16\times m\times n)\times 1)}\,, \tag{12}$$

with

$$[A(\omega)]_{((16\times m\times n)\times(42\times n+4))} = \begin{bmatrix} W(\omega_1) & [0]_{16\times m\times 42} & [0]_{16\times m\times 42} & \dots & R(\omega_1) \\ [0]_{16\times m\times 42} & W(\omega_2) & [0]_{16\times m\times 42} & \dots & R(\omega_2) \\ \vdots & \vdots & \ddots & \vdots & \vdots \\ [0]_{16\times m\times 42} & [0]_{16\times m\times 42} & \dots & W(\omega_n) & R(\omega_n) \end{bmatrix};$$

$$\{X(\omega)\}_{((42\times n+4)\times 1)} = \begin{Bmatrix} x(\omega_1) \\ x(\omega_2) \\ \vdots \\ x(\omega_n) \\ f \end{Bmatrix}; \qquad \{B(\omega)\}_{((16\times m\times n)\times 1)} = \begin{Bmatrix} b(\omega_1) \\ b(\omega_2) \\ \vdots \\ b(\omega_n) \end{Bmatrix},$$

where subscript n represents number of speeds considered for estimation. In Eq. (12), the regression matrix $[A(\omega)]$ has two components $[W(\omega)]$ and $[R(\omega)]$. The contributions from stiffness and damping of bearings and coupling and are stacked in $[W(\omega)]$ and contribution from residual unbalances are stacked in $[R(\omega)]$, respectively. The vector $\{X(\omega)\}$ contains all the unknown parameters, i.e., the speed–dependent stiffness and damping parameters of bearings and coupling, and the speed independent residual unbalances. The vector $\{B(\omega)\}$, have contributions from mass of rotor and the trial unbalances. To estimate unknown parameters, mathematical rearrangement can be performed on Eq. (12) and the least squares form could be obtained as

$$\{X(\omega)\}_{((42\times n+4)\times 1)} = \left([A(\omega)]^{\mathrm{T}}_{((42\times n+4)\times(16\times m\times n))}[A(\omega)]_{((16\times m\times n)\times(42\times n+4))}\right)^{-1} \times [A(\omega)]^{\mathrm{T}}_{((42\times n+4)\times(16\times m\times n))}\{B(\omega)\}_{((16\times m\times n)\times 1)}. \quad (13)$$

The numerical simulation to estimate speed-dependent dynamic parameters along with speed independent residual unbalances for the coupled rotor-bearing model as shown in Fig. 1 is discussed in the subsequent section.

With the help of estimated parameters (i.e., coupling dynamic parameters) evaluated from Eq. (13) and the corresponding displacements at coupling location, the misalignment forces in x and y directions and moments in (x–z) and (y–z) planes could be obtained by using equations derived by authors of [2] as follows,

$$\begin{aligned} F^{mis}_X &= k^c_{uu}(u^c_1 - u^c_2) + k^c_{uv}(v^c_1 - v^c_2); \\ F^{mis}_Y &= k^c_{vu}(u^c_1 - u^c_2) + k^c_{vv}(v^c_1 - v^c_2); \\ M^{mis}_{XZ} &= k^c_{\varphi_u}(\varphi^c_{v_1} - \varphi^c_{v_2}); \\ M^{mis}_{YZ} &= k^c_{\varphi_v}(\varphi^c_{u_1} - \varphi^c_{u_2}) \end{aligned} \quad (14)$$

where $(u^c_1,\ u^c_2)$ and $(v^c_1,\ v^c_2)$ are the linear displacements, $(\varphi^c_{u_1}, \varphi^c_{u_2})$ and $(\varphi^c_{v_1}, \varphi^c_{v_2})$ are the angular displacements at the coupling location in x and y directions at left and right side the of coupling, respectively, for one spin speed.

5. Numerical simulation

Numerical simulation is performed on MATLAB environment with system configuration as HP build CPU with 2GB RAM and Intel core i5 processor. An inbuilt solver Linsolve is used to solve the linear system of equations. A simple rotor-bearing-coupling system presented in Fig. 1 is considered for the numerical simulation. The rotor system consists of two massless rigid shafts each of length 1.25 m, mounted on two flexible bearings at ends and connected with a flexible coupling. Each shaft is having a thin rigid disc at mid of diametral moment of inertia and mass of (0.006 kg·m^2, 3 kg) and (0.016 kg·m^2, 6 kg), respectively. The magnitude and phase of residual unbalances for disc 1 and disc 2 are taken as (0.00586 kg·m, 36 deg.) and (0.00747 kg·m, 144 deg.), respectively. To generate the numerically-simulated response, stiffness and damping parameters of bearings and coupling at discrete frequencies (279 Hz and 281 Hz) and speed–independent residual unbalances are assumed. Assumed values of stiffness and damping coefficients of bearings and coupling and residual unbalances are given in Tables 1–7. The error calculated in Figs. 3–6 and Tables 1–7 is based on the deviation in values of estimated parameters form assumed values of parameters and are calculated as,

$$\% \text{ error} = \frac{\text{Assumed value} - \text{Estimated value}}{\text{Assumed value}} \times 100.$$

The estimation of unknown parameters for two different cases, i.e., *Case A* and *Case B*, are presented in the next section.

5.1. Case A: With three sets of measurement, i.e., exactly determined case

In this case, to make the system of equations exactly determined, minimum three independent sets of forced responses are required and generated as, for clockwise rotation: (i) without any trial unbalance (ii) with trial unbalance 1 (f_1^t) and for counter-clockwise rotation: (i) without any trial unbalance. Magnitudes and phase of the trial unbalance are taken as (0.01 kg·m and 90 deg.). Fig. 3 and Fig. 4, represent the percentage deviation in estimated parameters for different spin speeds, i.e., 279 Hz and 281 Hz, respectively. From Fig. 3 and Fig. 4, it could be observed that most of the estimated parameters exhibit well agreement with the assumed values for without noise condition, however, deviation increases with the addition of percentage noise. The maximum percentage error could be observed as (276, 331) and (230, 438) for 1% and 5% noise conditions, for 279 Hz and 281 Hz, respectively. From Fig. 3 and Fig. 4, it could be seen that maximum deviation occurred for cross coupled bearing damping parameter ($c_{uv}^{b_2}$).

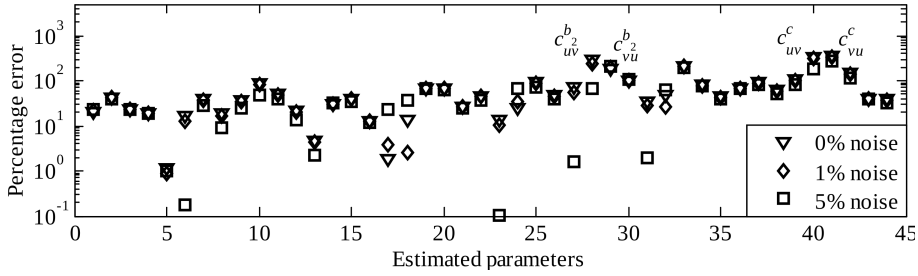

Fig. 3. Error plot of estimated parameters at 279 Hz for *Case A*

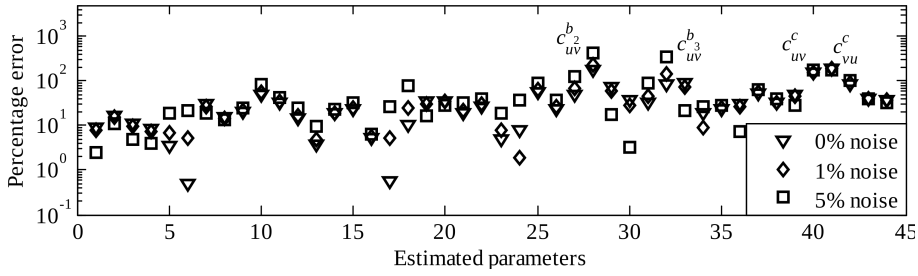

Fig. 4. Error plot of estimated parameters at 281 Hz for *Case A*

5.2. Case B: With more (eight) sets of measurement, i.e., highly over–determined case

For aforementioned case, to make the system of equations over–determined eight independent sets of forced response measurements are required and generated as, for clockwise rotation: (i) without any trial unbalance, (ii) with trial unbalance 1 (f_1^t), (iii) with trial unbalance 2 (f_2^t), (iv) with trial unbalance 3 (f_3^t). Magnitudes and phases of three trial unbalances are taken as (0.01 kg·m and 90 deg.), (0.02 kg·m and 60 deg.) and (0.03 kg·m and 90 deg.), respectively. Percentage deviation in estimated parameters for two different spin speeds, i.e., 279 Hz and 281 Hz are presented in Fig. 5 and Fig. 6, respectively. From Fig. 5 and Fig. 6, it could be observed that most of the estimated parameters exhibit well agreement with

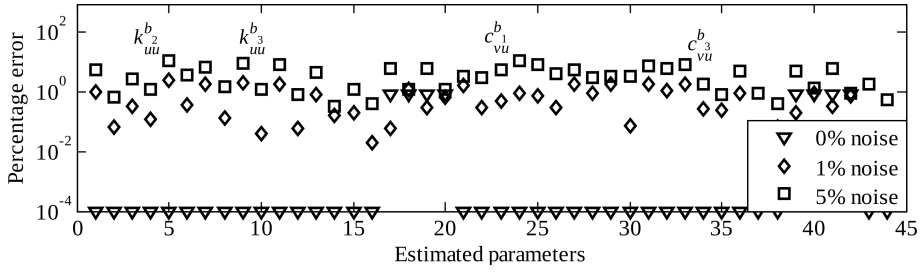

Fig. 5. Error plot of estimated parameters at 279 Hz for *Case B*

assumed values up to 5% noise condition. The maximum percentage error could be observed around (2, 11) and (2, 12) for 1% and 5% noise conditions, for 279 Hz and 281 Hz, respectively. Highest deviation could be seen for cross–coupled damping coefficient of bearing ($c^{b_1}_{vu}$) for 5% noise condition.

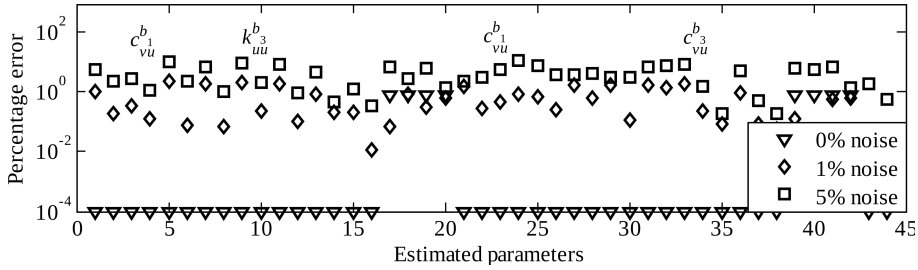

Fig. 6. Error plot of estimated parameters at 281 Hz for *Case B*

On comparison, from Figs. 3–6, it could be concluded that *Case B* is the best case of estimation. However, the accuracy can be further increased by analyzing equations independently using backward elimination process [27], in future. At present, for the best estimation case, i.e., *Case B*, speed–dependent estimated parameters and residual unbalances for different level of measurement noise (up to

Table 1.

Percentage deviation of speed–dependent bearing stiffness parameters at 279 Hz for *Case B*

Dynamic parameters	Assumed values	Estimated parameters					
		With 0% noise	Error	With 1% noise	Error	With 5% noise	Error
$k^{b_1}_{uu}$ (N/m)	250000	250000.00	0.00	247461.99	1.02	235969.90	5.61
$k^{b_1}_{uv}$ (N/m)	125000	125000.00	0.00	125086.64	0.07	124134.96	0.69
$k^{b_1}_{vu}$ (N/m)	140000	140000.00	0.00	139555.67	0.32	136072.25	2.80
$k^{b_1}_{vv}$ (N/m)	280000	280000.00	0.00	279645.97	0.13	276478.32	1.25
$k^{b_2}_{uu}$ (N/m)	250000	250000.00	0.00	256143.81	2.46	276965.27	10.79
$k^{b_2}_{uv}$ (N/m)	125000	125000.00	0.00	124548.55	0.36	120156.13	3.88
$k^{b_2}_{vu}$ (N/m)	140000	140000.00	0.00	142491.50	1.78	149318.90	6.66
$k^{b_2}_{vv}$ (N/m)	280000	280000.00	0.00	279614.87	0.14	275795.19	1.50
$k^{b_3}_{uu}$ (N/m)	300000	300000.00	0.00	293806.13	2.06	273218.86	8.93
$k^{b_3}_{uv}$ (N/m)	175000	175000.00	0.00	175070.74	0.04	177244.05	1.28
$k^{b_3}_{vu}$ (N/m)	190000	190000.00	0.00	186403.81	1.89	174450.56	8.18
$k^{b_3}_{vv}$ (N/m)	320000	320000.00	0.00	320197.72	0.06	322591.59	0.81
$k^{b_4}_{uu}$ (N/m)	300000	300000.00	0.00	302452.65	0.82	313976.80	4.66
$k^{b_4}_{uv}$ (N/m)	175000	175000.00	0.00	174712.47	0.16	174412.24	0.34
$k^{b_4}_{vu}$ (N/m)	190000	190000.00	0.00	190374.78	0.20	192432.18	1.28
$k^{b_4}_{vv}$ (N/m)	320000	320000.00	0.00	320062.22	0.02	321253.39	0.39

5%) are presented in Tables 1–7. From Fig. 5, Fig. 6 and Tables 1–7, it could be seen that the maximum percentage error for 5% noise condition is around ($c_{vu}^{b_1} = 11\%$) and ($c_{vu}^{b_1} = 12\%$) for 279 Hz and 281 Hz, respectively.

Table 2.
Percentage deviation of speed–dependent bearing damping parameters at 279 Hz for *Case B*

Dynamic parameters	Assumed values	Estimated parameters					
		With 0% noise	Error	With 1% noise	Error	With 5% noise	Error
$c_{uu}^{b_1}$(Ns/m)	305	305	0.00	303.46	0.50	287.30	5.80
$c_{uv}^{b_1}$(Ns/m)	112	112	0.00	110.94	0.95	99.30	11.34
$c_{vu}^{b_1}$(Ns/m)	114	114	0.00	113.17	0.73	104.35	8.46
$c_{vv}^{b_1}$(Ns/m)	310	310	0.00	309.06	0.30	296.80	4.26
$c_{uu}^{b_2}$(Ns/m)	305	305	0.00	310.75	1.89	321.47	5.40
$c_{uv}^{b_2}$(Ns/m)	112	112	0.00	113.02	0.91	108.56	3.07
$c_{vu}^{b_2}$(Ns/m)	114	114	0.00	116.10	1.84	117.80	3.34
$c_{vv}^{b_2}$(Ns/m)	310	310	0.00	309.77	0.08	299.76	3.30
$c_{uu}^{b_3}$(Ns/m)	290	290	0.00	284.53	1.89	267.35	7.81
$c_{uv}^{b_3}$(Ns/m)	120	120	0.00	121.29	1.07	127.69	6.41
$c_{vu}^{b_3}$(Ns/m)	125	125	0.00	122.69	1.85	114.12	8.70
$c_{vv}^{b_3}$(Ns/m)	295	295	0.00	295.79	0.27	300.27	1.79
$c_{uu}^{b_4}$(Ns/m)	290	290	0.00	289.30	0.24	287.59	0.83
$c_{uv}^{b_4}$(Ns/m)	120	120	0.00	118.89	0.93	113.94	5.04
$c_{vu}^{b_4}$(Ns/m)	125	125	0.00	125.06	0.05	123.81	0.95
$c_{vv}^{b_4}$(Ns/m)	295	295	0.00	294.80	0.07	293.84	0.39

Table 3.
Percentage deviation of speed–dependent coupling parameters at 279 Hz for *Case B*

Dynamic parameters	Assumed values	Estimated parameters					
		With 0% noise	Error	With 1% noise	Error	With 5% noise	Error
k_{uu}^{c}(N/m)	275000	277217.74	0.81	275160.96	0.06	257372.28	6.41
k_{uv}^{c}(N/m)	150000	151209.68	0.81	151790.97	1.19	148114.14	1.26
k_{vu}^{c}(N/m)	160000	161290.32	0.81	159542.30	0.29	150373.70	6.02
k_{vv}^{c}(N/m)	300000	302419.35	0.81	302094.59	0.70	296323.73	1.23
$k_{\varphi_u}^{c}$(N/m)	275000	275000.00	0.00	279582.52	1.67	284445.65	3.43
$k_{\varphi_v}^{c}$(N/m)	300000	300000.00	0.00	299096.88	0.30	290791.64	3.07
c_{uu}^{c}(Ns/m)	305	307.46	0.81	305.63	0.21	290.35	4.80
c_{uv}^{c}(Ns/m)	119	119.96	0.81	120.11	0.93	117.42	1.32
c_{vu}^{c}(Ns/m)	121	121.98	0.81	120.59	0.34	113.63	6.09
c_{vv}^{c}(Ns/m)	315	317.54	0.81	317.33	0.74	312.06	0.93

Table 4.

Percentage deviation of speed–dependent bearing stiffness parameters at 281 Hz for *Case B*

Dynamic parameters	Assumed values	Estimated parameters					
		With 0% noise	Error	With 1% noise	Error	With 5% noise	Error
$k_{uu}^{b_1}$ (N/m)	280000	280000.00	0.00	277093.97	1.04	263641.85	5.84
$k_{uv}^{b_1}$ (N/m)	140000	140000.00	0.00	139720.23	0.20	136674.73	2.38
$k_{vu}^{b_1}$ (N/m)	125000	125000.00	0.00	124554.95	0.36	121269.44	2.98
$k_{vv}^{b_1}$ (N/m)	250000	250000.00	0.00	249664.13	0.13	247065.87	1.17
$k_{uu}^{b_2}$ (N/m)	280000	280000.00	0.00	286810.50	2.43	309474.35	10.53
$k_{uv}^{b_2}$ (N/m)	140000	140000.00	0.00	139893.64	0.08	136628.21	2.41
$k_{vu}^{b_2}$ (N/m)	125000	125000.00	0.00	127386.83	1.91	134079.40	7.26
$k_{vv}^{b_2}$ (N/m)	250000	250000.00	0.00	249821.57	0.07	247365.98	1.05
$k_{uu}^{b_3}$ (N/m)	320000	320000.00	0.00	313246.51	2.11	290965.49	9.07
$k_{uv}^{b_3}$ (N/m)	190000	190000.00	0.00	190432.73	0.23	194010.01	2.11
$k_{vu}^{b_3}$ (N/m)	175000	175000.00	0.00	171650.91	1.91	160498.86	8.29
$k_{vv}^{b_3}$ (N/m)	300000	300000.00	0.00	300300.09	0.10	302853.12	0.95
$k_{uu}^{b_4}$ (N/m)	320000	320000.00	0.00	322684.52	0.84	335313.54	4.79
$k_{uv}^{b_4}$ (N/m)	190000	190000.00	0.00	189614.11	0.20	189113.64	0.47
$k_{vu}^{b_4}$ (N/m)	175000	175000.00	0.00	175352.52	0.20	177320.06	1.33
$k_{vv}^{b_4}$ (N/m)	300000	300000.00	0.00	300035.24	0.01	301086.47	0.36

Table 5.

Percentage deviation of speed–dependent bearing damping parameters at 281 Hz for *Case B*

Dynamic parameters	Assumed values	Estimated parameters					
		With 0% noise	Error	With 1% noise	Error	With 5% noise	Error
$c_{uu}^{b_1}$ (Ns/m)	300	300.00	0.00	298.59	0.47	282.11	5.96
$c_{uv}^{b_1}$ (Ns/m)	115	115.00	0.00	113.99	0.88	101.79	11.49
$c_{vu}^{b_1}$ (Ns/m)	110	110.00	0.00	109.26	0.67	101.36	7.85
$c_{vv}^{b_1}$ (Ns/m)	313	313.00	0.00	312.15	0.27	300.75	3.91
$c_{uu}^{b_2}$ (Ns/m)	300	300.00	0.00	304.96	1.65	312.11	4.04
$c_{uv}^{b_2}$ (Ns/m)	115	115.00	0.00	115.71	0.62	110.20	4.17
$c_{vu}^{b_2}$ (Ns/m)	110	110.00	0.00	111.86	1.69	113.30	3.00
$c_{vv}^{b_2}$ (Ns/m)	313	313.00	0.00	312.65	0.11	302.80	3.26
$c_{uu}^{b_3}$ (Ns/m)	390	390.00	0.00	383.49	1.67	362.20	7.13
$c_{uv}^{b_3}$ (Ns/m)	125	125.00	0.00	126.80	1.44	134.70	7.76
$c_{vu}^{b_3}$ (Ns/m)	129	129.00	0.00	126.54	1.91	117.53	8.89
$c_{vv}^{b_3}$ (Ns/m)	395	395.00	0.00	395.96	0.24	401.31	1.60
$c_{uu}^{b_4}$ (Ns/m)	390	390.00	0.00	389.68	0.08	389.27	0.19
$c_{uv}^{b_4}$ (Ns/m)	125	125.00	0.00	123.83	0.93	118.65	5.08
$c_{vu}^{b_4}$ (Ns/m)	129	129.00	0.00	129.11	0.09	128.33	0.52
$c_{vv}^{b_4}$ (Ns/m)	395	395.00	0.00	394.77	0.06	394.28	0.18

Table 6.

Percentage deviation of speed–dependent coupling parameters at 281 Hz for *Case B*

Dynamic parameters	Assumed values	Estimated parameters					
		With 0% noise	Error	With 1% noise	Error	With 5% noise	Error
k^c_{uu} (N/m)	300000	302419.35	0.81	299788.19	0.07	278864.91	7.05
k^c_{uv} (N/m)	160000	161290.32	0.81	161337.98	0.84	155456.12	2.84
k^c_{vu} (N/m)	150000	151209.68	0.81	149540.55	0.31	140876.39	6.08
k^c_{vv} (N/m)	275000	277217.74	0.81	276788.80	0.65	271025.41	1.45
$k^c_{\varphi_u}$ (N/m)	300000	300000.00	0.00	304523.32	1.51	307153.90	2.38
$k^c_{\varphi_v}$ (N/m)	275000	275000.00	0.00	274195.09	0.29	266431.67	3.12
c^c_{uu} (Ns/m)	307	309.48	0.81	306.60	0.13	287.72	6.28
c^c_{uv} (Ns/m)	117	117.94	0.81	116.95	0.04	110.49	5.56
c^c_{vu} (Ns/m)	125	126.01	0.81	124.31	0.55	116.17	7.06
c^c_{vv} (Ns/m)	318	320.56	0.81	319.97	0.62	313.52	1.41

Table 7.

Percentage deviation of unbalance parameters for *Case B*

Parameters	Assumed values	Estimated parameters					
		With 0% noise	Error	With 1% noise	Error	With 5% noise	Error
F^{res}_1 (kg·m)	$5.86{\cdot}10^{-3}$	$5.859{\cdot}10^{-3}$	0.00	$5.861{\cdot}10^{-3}$	0.03	$5.750{\cdot}10^{-3}$	1.86
F^{res}_2 (kg·m)	$7.47{\cdot}10^{-3}$	$7.469{\cdot}10^{-3}$	0.00	$7.468{\cdot}10^{-3}$	0.01	$7.427{\cdot}10^{-3}$	0.56

6. Conclusion

An insight discussion related to the development of an identification algorithm for simultaneous estimation of speed–dependent bearing and coupling dynamic parameters and residual unbalances is presented in this article. To estimate the parameters, two different cases (*Case A* and *B*) are analyzed and found that under *Case A*, regression matrix is highly ill–conditioned that leads to bad estimation, whereas *Case B* is the best case of estimation among the two, even with high level of percentage noise (up to 5%). Least squares technique is used to estimate the speed–dependent dynamic parameters and inherent unbalances. Different levels of measurement noise have been added to the developed algorithm and effects are discussed in the form of error plots. Estimates are found to be acceptable even with the addition of noise, although the least squares estimator is developed under the assumption of no noise condition. In the present developed algorithm, noise is deliberately added into the simulated response to mimic the actual test response. As the estimates are biased due to measurement noise in the registered signals, to increase accuracy of the estimates, the Output Error Method along

with least squares technique could be used to estimate the parameters [28]. Apart from least squares technique, some other identification technique such as Kalman Filter could be used as an identification algorithm to estimate the parameters, in future.

Appendix A: Matrices of equation of motion

A.1. Elements of mass matrix

$$M_{11} = M_{22} = M_{55} = M_{66} = \left(0.25m_1^d + \frac{I_1}{l^2}\right),$$
$$M_{12} = M_{21} = M_{56} = M_{65} = \left(0.25m_1^d - \frac{I_1}{l^2}\right),$$
$$M_{33} = M_{44} = M_{77} = M_{88} = \left(0.25m_2^d + \frac{I_2}{l^2}\right),$$
$$M_{34} = M_{43} = M_{78} = M_{87} = \left(0.25m_2^d - \frac{I_2}{l^2}\right).$$

A.2. Damping matrix

$$[C] = \begin{bmatrix} c_{uu}^{b_1} + 0.062c_{uu}^c & -0.312c_{uu}^c & 0.312c_{uu}^c & -0.062c_{uu}^c & c_{vu}^{b_1} + 0.062c_{vu}^c & -0.312c_{uv}^c & 0.312c_{uv}^c & -0.062c_{uv}^c \\ -0.312c_{uu}^c & c_{uu}^{b_2} + 1.562c_{uu}^c & -1.562c_{uu}^c & 0.312c_{uu}^c & -0.312c_{vu}^c & c_{uv}^{b_2} + 1.562c_{uv}^c & -1.562c_{uv}^c & 0.312c_{uv}^c \\ 0.312c_{uu}^c & -1.562c_{uu}^c & c_{uu}^{b_3} + 1.562c_{uu}^c & -0.312c_{uu}^c & 0.312c_{vu}^c & -1.562c_{uv}^c & c_{uv}^{b_3} + 1.562c_{uv}^c & -0.312c_{uv}^c \\ -0.062c_{uu}^c & 0.312c_{uu}^c & -0.312c_{uu}^c & c_{uu}^{b_4} + 0.062c_{uu}^c & -0.062c_{vu}^c & 0.312c_{uv}^c & -0.312c_{uv}^c & c_{vu}^{b_4} + 0.062c_{uv}^c \\ c_{vv}^{b_1} + 0.062c_{vu}^c & -0.312c_{vu}^c & 0.312c_{vu}^c & -0.062c_{vu}^c & c_{vv}^{b_1} + 0.062c_{vv}^c & -0.312c_{vv}^c & 0.312c_{vv}^c & -0.062c_{vv}^c \\ -0.312c_{vu}^c & c_{vv}^{b_2} + 1.562c_{vu}^c & -1.562c_{vu}^c & 0.312c_{vu}^c & -0.312c_{vv}^c & c_{vv}^{b_2} + 1.562c_{vv}^c & -1.562c_{vv}^c & 0.312c_{vv}^c \\ 0.312c_{vu}^c & -1.562c_{vu}^c & c_{vv}^{b_3} + 1.562c_{vu}^c & -0.312c_{vu}^c & 0.312c_{vv}^c & -1.562c_{vv}^c & c_{vv}^{b_3} + 1.562c_{vv}^c & -0.312c_{vv}^c \\ -0.062c_{vu}^c & 0.312c_{vu}^c & -0.312c_{vu}^c & c_{vv}^{b_4} + 0.062c_{vu}^c & -0.062c_{vv}^c & 0.312c_{vv}^c & -0.312c_{vv}^c & c_{vv}^{b_4} + 0.062c_{vv}^c \end{bmatrix}.$$

A.3. Stiffness matrix

$$[K] = \begin{bmatrix} k_{uu}^{b_1}+ak_{uu}^c+dk_{\varphi_v}^c & -bk_{uu}^c-dk_{\varphi_v}^c & bk_{uu}^c+dk_{\varphi_v}^c & -ak_{uu}^c-dk_{\varphi_v}^c & k_{uv}^{b_1}+ak_{uv}^c & -bk_{uv}^c & bk_{uv}^c & ak_{uv}^c \\ -bk_{uu}^c-dk_{\varphi_v}^c & k_{uu}^{b_2}+ck_{uu}^c+dk_{\varphi_v}^c & -ck_{uu}^c-ek_{\varphi_v}^c & bk_{uu}^c+ek_{\varphi_v}^c & -bk_{uv}^c & k_{uv}^{b_2}+ck_{uv}^c & -ck_{uv}^c & bk_{uv}^c \\ bk_{uu}^c+ek_{\varphi_v}^c & -ck_{uu}^c-ek_{\varphi_v}^c & k_{uu}^{b_3}+ck_{uu}^c+fk_{\varphi_v}^c & -bk_{uu}^c-fk_{\varphi_v}^c & bk_{uv}^c & -ck_{uv}^c & k_{uv}^{b_3}+ck_{uv}^c & -bk_{uv}^c \\ -ak_{uu}^c-ek_{\varphi_v}^c & bk_{uu}^c+ek_{\varphi_v}^c & -bk_{uu}^c-fk_{\varphi_v}^c & k_{uu}^{b_4}+ak_{uu}^c+fk_{\varphi_v}^c & -ak_{uv}^c & bk_{uv}^c & -bk_{uv}^c & k_{uv}^{b_4}+ak_{uv}^c \\ k_{vu}^{b_1}+ak_{vu}^c & -bk_{vu}^c & bk_{vu}^c & ak_{vu}^c & k_{vv}^{b_1}+ak_{vv}^c+dk_{\varphi_u}^c & -bk_{vv}^c-dk_{\varphi_u}^c & bk_{vv}^c+dk_{\varphi_u}^c & -ak_{vv}^c-dk_{\varphi_u}^c \\ -bk_{vu}^c & k_{vu}^{b_2}+ck_{vu}^c & -ck_{vu}^c & bk_{vu}^c & -bk_{vv}^c-dk_{\varphi_u}^c & k_{vv}^{b_2}+ck_{vv}^c+dk_{\varphi_u}^c & -ck_{vv}^c-ek_{\varphi_u}^c & bk_{vv}^c+ek_{\varphi_u}^c \\ bk_{vu}^c & -ck_{vu}^c & k_{vu}^{b_3}+ck_{vu}^c & -bk_{vu}^c & bk_{vv}^c+ek_{\varphi_u}^c & -ck_{vv}^c-ek_{\varphi_u}^c & k_{vv}^{b_3}+ck_{vv}^c+fk_{\varphi_u}^c & -bk_{vv}^c-fk_{\varphi_u}^c \\ -ak_{vu}^c & bk_{vu}^c & -bk_{vu}^c & k_{vu}^{b_4}+ak_{vu}^c & -ak_{vv}^c-ek_{\varphi_u}^c & bk_{yy}^c+ek_{\varphi_u}^c & -bk_{vv}^c-fk_{\varphi_u}^c & k_{vv}^{b_4}+ak_{vv}^c+fk_{\varphi_u}^c \end{bmatrix}$$

$$a = \frac{1}{16}, \quad b = \frac{5}{16}, \quad c = \frac{25}{16}, \quad d = \frac{1}{l_1^2}, \quad e = \frac{1}{l_1 l_2}, \quad f = \frac{1}{l_2^2}$$

Appendix B: Matrices of regression equation in complex form

B.1. Elements of regression matrix corresponding to stiffness

$$K^R_{11} = u^b_1, \quad K^R_{12} = v^b_1, \quad K^R_{1,18} = K^R_{5,19} = 0.062(u^b_1 - 5u^b_2 + 5u^b_3 - u^b_4),$$
$$K^R_{1,18} = K^R_{5,20} = 0.062(v^b_1 - 5v^b_2 + 5v^b_3 - v^b_4), \quad K^R_{25} = u^b_2,$$
$$K^R_{26} = v^b_2, \quad K^R_{2,17} = K^R_{6,19} = 0.062(-5u^b_1 + 25u^b_2 - 25u^b_3 + 5u^b_4),$$
$$K^R_{2,18} = K^R_{6,20} = 0.062(-5v^b_1 + 25v^b_2 - 25v^b_3 + 5v^b_4), \quad K^R_{39} = u^b_3,$$
$$K^R_{3,10} = v^b_3, \quad K^R_{3,17} = K^R_{7,19} = 0.062(5u^b_1 - 25u^b_2 + 25u^b_3 - 5u^b_4),$$
$$K^R_{3,18} = K^R_{7,20} = 0.062(5v^b_1 - 25v^b_2 + 25v^b_3 - 5v^b_4), \quad K^R_{4,13} = u^b_4,$$
$$K^R_{4,14} = v^b_4, \quad K^R_{4,17} = K^R_{8,19} = 0.062(-u^b_1 + 5u^b_2 - 5u^b_3 + u^b_4),$$
$$K^R_{4,18} = K^R_{8,20} = 0.062(-v^b_1 + 5v^b_2 - 5v^b_3 + v^b_4), \quad K^R_{53} = u^b_1,$$
$$K^R_{54} = v^b_2, \quad K^R_{67} = u^b_2, \quad K^R_{68} = v^b_2, \quad K^R_{7,11} = u^b_3,$$
$$K^R_{7,12} = v^b_3, \quad K^R_{8,15} = u^b_4, \quad K^R_{8,16} = v^b_4,$$
$$K^R_{1,21} = \left(\frac{u^b_1 - u^b_2 + u^b_3 - u^b_4}{l^2}\right), \quad K^R_{2,21} = \left(\frac{u^b_2 - u^b_1 + u^b_4 - u^b_3}{l^2}\right),$$
$$K^R_{3,21} = \left(\frac{u^b_1 - u^b_2 + u^b_3 - u^b_4}{l^2}\right), \quad K^R_{4,21} = \left(\frac{u^b_2 - u^b_1 + u^b_4 - u^b_3}{l^2}\right),$$
$$K^R_{5,22} = \left(\frac{v^b_1 - v^b_2 + v^b_3 - v^b_4}{l^2}\right), \quad K^R_{6,22} = \left(\frac{v^b_2 - v^b_1 + v^b_4 - v^b_3}{l^2}\right),$$
$$K^R_{7,22} = \left(\frac{v^b_1 - v^b_2 + v^b_3 - v^b_4}{l^2}\right), \quad K^R_{8,22} = \left(\frac{v^b_2 - v^b_1 + v^b_4 - v^b_3}{l^2}\right).$$

B.2. Elements of regression matrix corresponding to damping

$$C^R_{11} = -j\omega u^b_1, \quad C^R_{12} = -j\omega v^b_1, \quad C^R_{25} = -j\omega u^b_2, \quad C^R_{26} = -j\omega v^b_2,$$
$$C^R_{39} = -j\omega u^b_3, \quad C^R_{3,10} = -j\omega v^b_3, \quad C^R_{4,13} = -j\omega u^b_4, \quad C^R_{4,14} = -j\omega v^b_4,$$
$$C^R_{53} = -j\omega u^b_1, \quad C^R_{54} = -j\omega v^b_1, \quad C^R_{67} = -j\omega u^b_2, \quad C^R_{68} = -j\omega v^b_2,$$
$$C^R_{7,11} = -j\omega u^b_3, \quad C^R_{7,12} = -j\omega v^b_3, \quad C^R_{8,15} = -j\omega u^b_4, \quad C^R_{8,16} = -j\omega v^b_4,$$
$$C^R_{1,17} = C^R_{5,19} = -0.062j\omega(u^b_1 - 5u^b_2 + 5u^b_3 - u^b_4),$$
$$C^R_{1,18} = C^R_{5,20} = -0.062j\omega(v^b_1 - 5v^b_2 + 5v^b_3 - v^b_4),$$
$$C^R_{2,17} = C^R_{6,19} = -0.062j\omega(-5u^b_1 + 25u^b_2 - 25u^b_3 + 5u^b_4),$$

$$
\begin{aligned}
C^R_{2,18} &= C^R_{6,20} = -0.062j\omega(-5v^b_1 + 25v^b_2 - 25v^b_3 + 5v^b_4),\\
C^R_{3,17} &= C^R_{7,19} = -0.062j\omega(5u^b_1 - 25u^b_2 + 25u^b_3 - 5u^b_4),\\
C^R_{3,18} &= C^R_{7,20} = -0.062j\omega(5v^b_1 - 25v^b_2 + 25v^b_3 - 5v^b_4),\\
C^R_{4,17} &= C^R_{8,19} = -0.062j\omega(-u^b_1 + 5u^b_2 - 5u^b_3 + u^b_4),\\
C^R_{4,18} &= C^R_{8,20} = -0.062j\omega(-v^b_1 + 5v^b_2 - 5v^b_3 + v^b_4),
\end{aligned}
$$

B.3. Elements of regression matrix corresponding to residual unbalance

$$
\begin{aligned}
F^R_{11} &= 0.50\omega^2 F^{res}_1 e^{j\phi_1}, & F^R_{21} &= 0.50\omega^2 F^{res}_1 e^{j\phi_1},\\
F^R_{32} &= 0.50\omega^2 F^{res}_2 e^{j\phi_2}, & F^R_{42} &= 0.50\omega^2 F^{res}_2 e^{j\phi_2},\\
F^R_{41} &= -0.50j\omega^2 F^{res}_1 e^{j\phi_1}, & F^R_{51} &= -0.50j\omega^2 F^{res}_1 e^{j\phi_1},\\
F^R_{62} &= -0.50j\omega^2 F^{res}_2 e^{j\phi_2}, & F^R_{72} &= -0.50j\omega^2 F^{res}_2 e^{j\phi_2}.
\end{aligned}
$$

B.4. Regression matrix corresponding to disc mass and trial unbalances

$$
\{B\} = \begin{Bmatrix}
0.25m^d_1 u^b_1 + \left(\frac{I_1}{l^2}\right) u^b_1 + 0.25m^d_1 u^b_2 - \left(\frac{I_1}{l^2}\right) u^b_2 + 0.50 f^t_1 e^{j\theta}\\
0.25m^d_1 u^b_1 - \left(\frac{I_1}{l^2}\right) u^b_1 + 0.25m^d_1 u^b_2 + \left(\frac{I_1}{l^2}\right) u^b_2 + 0.50 f^t_1 e^{j\theta}\\
0.25m^d_2 u^b_3 + \left(\frac{I_2}{l^2}\right) u^b_3 + 0.25m^d_2 u^b_4 - \left(\frac{I_2}{l^2}\right) u^b_4\\
0.25m^d_2 u^b_3 - \left(\frac{I_2}{l^2}\right) u^b_3 + 0.25m^d_2 u^b_4 + \left(\frac{I_2}{l^2}\right) u^b_4\\
0.25m^d_1 v^b_1 + \left(\frac{I_1}{l^2}\right) v^b_1 + 0.25m^d_1 v^b_2 - \left(\frac{I_1}{l^2}\right) v^b_2 - 0.50j f^t_1 e^{j\theta}\\
0.25m^d_1 v^b_1 - \left(\frac{I_1}{l^2}\right) v^b_1 + 0.25m^d_1 v^b_2 + \left(\frac{I_1}{l^2}\right) v^b_2 - 0.50j f^t_1 e^{j\theta}\\
0.25m^d_2 v^b_3 + \left(\frac{I_2}{l^2}\right) v^b_3 + 0.25m^d_2 v^b_4 - \left(\frac{I_2}{l^2}\right) v^b_4\\
0.25m^d_2 v^b_3 - \left(\frac{I_2}{l^2}\right) v^b_3 + 0.25m^d_2 v^b_4 + \left(\frac{I_2}{l^2}\right) v^b_4
\end{Bmatrix}
$$

Manuscript received by Editorial Board, February 16, 2018;
final version, July 02, 2018.

References

[1] A.T. Tadeo, K.L. Cavalca, and M.J. Brennan. Dynamic characterization of a mechanical coupling for a rotating shaft. *Proceedings of the Institution of Mechanical Engineers Part C: Journal of Mechanical Engineering Science*, 225(3):604–616, 2011. doi: 10.1243/09544062JMES2214.

[2] M. Lal and R. Tiwari. Quantification of multiple fault parameters in flexible turbo–generator systems with incomplete rundown vibration data. *Mechanical Systems and Signal Processing*, 41(1-2):546–563, 2013. doi: 10.1016/j.ymssp.2013.06.025.

[3] R. Tiwari, A.W. Lees, and M.I. Friswell. Identification of speed–dependent bearing parameters. *Journal of Sound and Vibration*, 254(5):967–986, 2002. doi: 10.1006/jsvi.2001.4140.

[4] K.M. Al-Hussain and I. Redmond. Dynamic response of two rotors connected by rigid mechanical coupling with parallel misalignment. *Journal of Sound and Vibration*, 249(3):483–498, 2002. doi: 10.1006/jsvi.2001.3866.

[5] K.M. Al-Hussain. Dynamic stability of two rigid rotors connected by a flexible coupling with angular misalignment. *Journal of Sound and Vibration*, 266(2):217–234, 2003. doi: 10.1016/S0022-460X(02)01627-9.

[6] R. Tiwari. Conditioning of regression matrices for simultaneous estimation of the residual unbalance and bearing dynamic parameters. *Mechanical Systems and Signal Processing*, 19(5):1082–1095, 2005. doi: 10.1016/j.ymssp.2004.09.005.

[7] R. Tiwari and V. Chakravarthy. Simultaneous identification of residual unbalances and bearing dynamic parameters from impulse responses of rotor–bearing systems. *Mechanical Systems and Signal Processing*, 20(7):1590–1614, 2006. doi: 10.1016/j.ymssp.2006.01.005.

[8] P. Jayaswal, A.K. Wadhwani, and K.B. Mulchandani. Machine fault signature analysis. *International Journal of Rotating Machinery*, 1–10, 2008. doi: 10.1155/2008/583982.

[9] A.K. Jalan and A.R. Mohanty. Model based fault diagnosis of a rotor–bearing system for misalignment and unbalance under steady–state condition. *Journal of Sound and Vibration*, 327(3-5): 604–622, 2009. doi: 10.1016/j.jsv.2009.07.014.

[10] A.W. Lees, J.K. Sinha, and M.I. Friswell. Model–based identification of rotating machines. *Mechanical Systems and Signal Processing*, 23(6):1884–1893, 2009. doi: 10.1016/j.ymssp.2008.08.008.

[11] C.Y. Tsai and S.C. Huang. Transfer matrix for rotor coupler with parallel misalignment. *Journal of Mechanical Science and Technology*, 23(5):1383–1395, 2009. doi: 10.1007/s12206-008-1216-9.

[12] J. Jing and G. Meng. A novel method for multi-fault diagnosis of rotor system. *Mechanism and Machine Theory*, 44(4):697–709, 2009. doi: 10.1016/j.mechmachtheory.2008.05.002.

[13] T.H. Patel and A.K. Darpe. Vibration response of misaligned rotors. *Journal of Sound and Vibration*, 325(3):609–628, 2009. doi: 10.1016/j.jsv.2009.03.024.

[14] T.H. Patel and A.K. Darpe. Experimental investigations on vibration response of misaligned rotors. *Mechanical Systems and Signal Processing*, 23(7):2236–2252, 2009. doi: 10.1016/j.ymssp.2009.04.004.

[15] S. Sarkar, A. Nandi, S. Neogy, J.K. Dutt, and T.K. Kundra. Finite element analysis of misaligned rotors on oil-film bearings. *Sadhana*, 35(1):45–61, 2010. doi: 10.1007/s12046-010-0005-1.

[16] Q.W. Yang. A new damage identification method based on structural flexibility disassembly. *Journal of Vibration and Control*, 17(7):1000–1008, 2011. doi: 10.1177/1077546309360052.

[17] G.N.D.S. Sudhakar and A.S. Sekhar. Identification of unbalance in a rotor bearing system. *Journal of Sound and Vibration*, 330(10):2299–2313, 2011. doi: 10.1016/j.jsv.2010.11.028.

[18] S. Ganesan and C. Padmanabhan. Modelling of parametric excitation of a flexible coupling–rotor system due to misalignment. *Proceedings of the Institution of Mechanical Engineers, Part C: Journal of Mechanical Engineering Science*, 225(12):2907–2918, 2011. doi: 10.1177/0954406211411549.

[19] M. Lal and R. Tiwari. Multi–fault identification in simple rotor–bearing–coupling systems based on forced response measurements. *Mechanism and Machine Theory*, 51:87–109, 2012. doi: 10.1016/j.mechmachtheory.2012.01.001.

[20] M. Lal and R. Tiwari. Identification of multiple faults with Incomplete response measurements in rotor-bearing-coupling systems. In *ASME 2012 Gas Turbine India Conference*, pages 613–620, Mumbai, India, 1 December 2012. doi: 10.1115/GTINDIA2012-9542.

[21] M. Lal and R. Tiwari. Identification of multiple fault parameters in a rigid-rotor and flexible-bearing-coupling system: An experimental investigation. In *ASME 2013 Gas Turbine India* Conference, Bangalore, India, 5–6, December 2013. doi: 10.1115/GTINDIA2013-3774.

[22] M. Lal and R. Tiwari. Experimental estimation of misalignment effects in rotor-bearing-coupling systems. In *Proceedings of the 9th IFToMM International Conference on Rotor Dynamics*, pages 779–789, Springer, 2015. doi: 10.1007/978-3-319-06590-8_64.

[23] M. Lal and R. Tiwari. Experimental identification of shaft misalignment in a turbo-generator system. *Sadhana*, 43:80, 2018. doi: 10.1007/s12046-018-0859-1.

[24] P. Pennacchi, A. Vania, and S. Chatterton. Nonlinear effects caused by coupling misalignment in rotors equipped with journal bearings. *Mechanical Systems and Signal Processing*, 30:306–322, 2012. doi: 10.1016/j.ymssp.2011.11.020.

[25] Y. Lei, J. Lin, Z. He, and M.J. Zuo. A review on empirical mode decomposition in fault diagnosis of rotating machinery. *Mechanical Systems and Signal Processing*, 35(1-2):108–126, 2013. doi: doi.org/10.1016/j.ymssp.2012.09.015.

[26] S.K. Kuppa and M. Lal. Characteristic parameter estimation of AMB supported coupled rotor system. In *ASME 2017 Gas Turbine India Conference*, Bangalore, India, 7–8 December, 2017. doi: 10.1115/GTINDIA2017-4641.

[27] R.V. Jategaonkar. *Flight Vehicle System Identification: A Time-Domain Methodology*. 2nd edition, AIAA, Reston, Virginia, 2015. doi: 10.2514/4.102790.

[28] P. Lichota, J. Szulczyk, D.A. Norena, and F.A. Vallejo Monsalve. Power spectrum optimization in the design of multisine manoeuvre for identification purposes, *Journal of Theoretical and Applied Mechanics*, 55(4):1193–1203, 2017. doi: 10.15632/jtam-pl.55.4.1193.